Journal of Intelligent Material Systems and Structures
http://jim.sagepub.com

Structural Health Monitoring using ARMarkov Observers

Prasad Dharap, Bong-Hwan Koh and Satish Nagarajaiah

Journal of Intelligent Material Systems and Structures 2006; 17; 469
DOI: 10.1177/1045389X06058793

The online version of this article can be found at:
http://jim.sagepub.com/cgi/content/abstract/17/6/469

Published by:
SAGE Publications
http://www.sagepublications.com

Structural Health Monitoring using ARMarkov Observers

PRASAD DHARAP,[1] BONG-HWAN KOH[2,*] AND SATISH NAGARAJAIAH[3,†]

[1]*Department of Civil and Environmental Engineering*
Rice University, Houston, TX 77005, USA

[2]*Department of Mechanical Engineering, Dohgguk University*
Seoul, 100-715, Republic of Korea

[3]*Departments of Civil and Environmental Engineering and*
Mechanical Engineering and Material Sciences
Rice University, Houston, TX 77005, USA

ABSTRACT: A new method based on a bank of ARMarkov observers is proposed in this study for determination of the extent of damage. The objective of this article is to present a new formulation using a predesigned set of ARMarkov observers to determine the extent of damage and track further changes in the stiffness of the damaged member. The primary advantages of the proposed formulation over the existing methods are: (1) ARMarkov observers are designed based on interaction matrix formulation so that knowledge about exact initial conditions is not necessary, and (2) noise statistics are not required *a priori* to design a bank of ARMarkov observers when compared to a bank of Kalman filters. The simulation results of several examples including a planar truss structure with progressive damage in a member are presented to highlight the capability of the proposed method. The proposed method works well in the case of either a full set or a limited number of available measurements. It is shown that sensitivity enhancing control (SEC) can be easily incorporated into the proposed method to enhance the sensitivity of structural damage. In case of noisy output measurements, it is shown that it is possible to distinguish between the errors due to structural damage and due to noise in output measurements.

Key Words: online structural health monitoring, SEC, ARMarkov observers, interaction matrix.

INTRODUCTION

STRUCTURAL health monitoring has been the topic of recent study by a number of researchers. Rytter (1993) has broadly categorized damage identification into four levels: (1) Level 1 – determination that damage is present in a structure; (2) Level 2 – determination of the geometric location of the damage; (3) Level 3 – quantification of the severity of the damage; and (4) Level 4 – prediction of the remaining service life of the structure. From the safety point of view, it is very important to determine the location and extent of damage at the earliest, at the onset of damage if possible, so that proper measures can be taken to avoid the failure of the whole system (Hjelmstad and Shin, 1995). Depending upon the safety margins used in the analysis and design of such systems, damaged structures can continue to serve the purpose without compromising safety considerations in civil and mechanical engineering structures. It is necessary to track the changes in stiffness of critical members in a structure in real time as exceeding a certain level of damage posing safety hazards and may need immediate attention.

Doebling et al. (1996) have done a literature survey on damage identification and health monitoring of structural and mechanical systems from changes in their vibration characteristics. Vibration based damage detection methods are preferred because visual inspection methods are generally costly, *a priori* knowledge about the vicinity of the damage has to be known, all components need to be readily accessible for visual inspection, and experience is necessary to make a reliable decision about the health of a structure (Doebling et al., 1996). Vibration based structural damage detection methods can be broadly categorized into frequency domain methods and time domain methods. Frequency domain methods are primarily modal analysis methods where natural frequencies (Adams et al., 1978; Armon et al., 1994), mode shapes

*Formerly, Department of Civil and Environmental Engineering, Rice University, Houston, TX 77005, USA.
†Author to whom correspondence should be addressed.
E-mail: nagaraja@rice.edu
Figures 3–14 appear in color online: http://jim.sagepub.com

1045-389X/06/06 0469–13 $10.00/0 DOI: 10.1177/1045389X06058793

or mode shape curvature (Hjelmstad and Shin, 1995; Stubbs et al., 1995; Cornwell et al., 1998), or some combination of frequency and mode shape information (Kam and Lee, 1992) of the structures is compared before and after damage and a quantitative analysis is performed so that the location and extent of damage can be determined. Using *a priori* knowledge of how certain damage scenarios affect modal properties, the correlation between measured modal frequency shifts and predicted modal frequency shifts for a given set of damage scenarios is used to identify damage location in forward methods. Inverse or model updating methods attempt to update mass and/or stiffness matrices of structural models based on measured modal frequencies and mode shapes. The resulting perturbation matrices indicate damage location. Accurate mode shape information is very difficult to obtain as the measurements are often corrupted by measurement error and noise. Another problem with modal analysis methods is the sensitivity of modal characteristics to small changes in structural characteristics. In addition, modal analysis methods are basically offline methods as the data acquisition and transformation from time domain to frequency domain needs to be performed before any quantitative analysis, though there are recursive estimation techniques for real time modal parameter identification (Tasker et al., 1999). For online structural health monitoring, time domain methods are preferred over modal analysis methods.

Time domain methods exploit the fact that the response of the damaged structure is different from that of the healthy structure. Comparing the damaged structure's response with the healthy structure's response indicates damage in a structure. However, it is still a challenge to determine the location and extent of damage. Input–output uncoupling is obtained using interaction matrix formulation (Koh et al., 2005a), where failure among the actuators is identified and isolated in real time. In another study, an interaction matrix based formulation has been developed (Koh et al., 2005b) for structural damage detection and was shown that it is possible to localize damage in a structure in real time. The authors treat structural damage in a member as an extra input force at the nodes, connecting the damaged member, to determine the location of damage (Level 1 and Level 2) in real time; although, no solution regarding how to determine the extent of damage (Level 3) in a member has been proposed.

Model based observers were first used by Beard (1971) and Jones (1973) as failure detection filters. With proper choice of filter feedback gains, these first-order model based observers predict outputs, which can identify and locate system component failures. Liberatore et al. (2003) have used a fault detection filter for structural health monitoring, specifically for a simply supported beam; fault direction vectors obtained from predefined damage locations in the structure were used as the basis for identification for each of the possible fault locations. Kranock (2000) has used model based state space observers, as structural damage detection filters and parameterized the feedback gain for damage localization. In this study, the authors have treated forces resulting from damage as inputs to the system and filter output indicating structural damage as well as location of damage in real time. A damage detection method for rotor dynamic system developed by Seibold and Weinert (1996) is based on Kalman filter bank. Kalman filter is an optimal state estimator, given a known model of the system under the influence of process and measurement noise with known statistics specified in terms of their covariance. In this filter bank approach, each filter represents a specific damage scenario and the crack is localized by examining the whiteness of estimation residual or innovation. To design Kalman filter bank, information about the measurement noise as well as system uncertainties is required *a priori*. However, in practice neither the process nor the noise statistics are known exactly.

Lim and Phan (1997) have used ARMarkov models, based on the concept of interaction matrix, for predictive control, where a multistep-ahead prediction of the system controlled response is used to make a current control decision. Interaction matrix formulation has applications ranging from state estimation (Lim et al., 1998), system and disturbance identification (Goodzeit and Phan, 2000), vibration suppression, disturbance rejection, tracking by predictive control (Phan et al., 1998; Darling and Phan, 2004a, b), actuator failure detection (Koh et al., 2005a), and real time structural damage localization (Koh et al., 2005b).

To date, multistep-ahead observer (Lim et al., 1998), referred to as ARMarkov observer in this article, has been used only for estimation problems and has not been applied for structural damage detection. In particular, the proposed method to determine the extent of damage based on a bank of ARMarkov observers has not been reported in the literature. In this article, a new formulation based on a filter bank of ARMarkov observers, incorporating estimated properties of damaged members, is proposed to determine the extent of damage (Level 3) and to track the stiffness variation in each damaged member. The proposed method overcomes the limitation of Kalman filter bank approach in which process and noise statistics are required *a priori*. In addition, knowledge of exact initial conditions is not necessary in ARMarkov observers when compared to state space observers, which is explained in greater detail in the next section.

The formulation for ARMarkov observers is presented in the next section where ARMarkov observers for q step-ahead prediction are designed from the known analytical model. Also presented is a formulation where

ARMarkov observers are designed from known input–output data. A three degree-of-freedom (DOF) spring–mass–damper example is presented. The results using ARMarkov observers are compared with the observer designed from the known state space analytical model. The error functions are computed by comparing the predicted output using ARMarkov observers and output measurements. The covariance of the error function is proposed as a parameter to evaluate the potential of ARMarkov observers to determine the extent of damage, although other parameters of the error function can also be used. It is shown that the proposed method performs well for structural health monitoring even in multiple damage scenarios. Noise in the output measurement is considered and by adjusting prediction horizon of the ARMarkov observer, it is possible to differentiate between the errors due to noise in output measurements and due to structural damage. Issues regarding the sensitivity to the small structural damage are discussed and it is shown that feedback control algorithms can easily be incorporated into the presented method to enhance the sensitivity of the structural damage. Finally, simulation results on planar truss structures are presented to validate the proposed method.

MATHEMATICAL FORMULATION

The formulation for designing an ARMarkov observer (Lim et al., 1998) for q step-ahead prediction from the known analytical model is presented here for the sake of completion.

Consider a nth order, r-input, m-output discrete-time model of a system in state space format

$$\begin{aligned} x(k+1) &= Ax(k) + Bu(k) \\ y(k) &= Cx(k) + Du(k) \end{aligned} \tag{1}$$

For $k=1$

$$\begin{aligned} x(2) &= Ax(1) + Bu(1) \\ y(1) &= Cx(1) + Du(1) \end{aligned} \tag{2}$$

For $k=2$

$$\begin{aligned} x(3) &= Ax(2) + Bu(2) \\ y(2) &= Cx(2) + Du(2) \end{aligned} \tag{3}$$

Substituting $x(2)$ from Equation (2)

$$\begin{aligned} x(3) &= A^2x(1) + ABu(1) + Bu(2) \\ y(2) &= CAx(1) + CBu(1) + Du(2) \end{aligned} \tag{4}$$

By repeated substitution, for some $p \geq 0$

$$\begin{aligned} x(k+p) &= A^p x(k) + C_{\text{ont}_p} u_p(k) \\ y_p(k) &= O_{\text{bs}_p} x(k) + T_{\text{op}_p} u_p(k) \end{aligned} \tag{5}$$

where

$$y_p(k) = \begin{bmatrix} y(k) \\ y(k+1) \\ \vdots \\ y(k+p-1) \end{bmatrix}, \quad u_p(k) = \begin{bmatrix} u(k) \\ u(k+1) \\ \vdots \\ u(k+p-1) \end{bmatrix} \tag{6}$$

For sufficiently large p, C_{ont_p} is an $n \times pr$ controllability matrix, O_{bs_p} is an $pm \times n$ observability matrix, T_{op_p} is an $pm \times pr$ Toeplitz matrix of the system of Markov parameters. Here, subscripts ont, bs, and op are used to denote controllability matrix, observability matrix, and Toeplitz matrix, respectively. Sub subscript like p and q are used to denote the order of matrices.

$$\begin{aligned} C_{\text{ont}_p} &= \left[A^{p-1}B, \ldots, AB, B\right], \\ O_{\text{bs}_p} &= \begin{bmatrix} C \\ CA \\ \vdots \\ CA^{p-1} \end{bmatrix} \\ \text{and} \quad T_{\text{op}_p} &= \begin{bmatrix} D & 0 & 0 & \cdots & 0 \\ CB & D & \ddots & \ddots & \vdots \\ CAB & CB & D & \ddots & 0 \\ \vdots & \ddots & \ddots & \ddots & 0 \\ CA^{p-2}B & \cdots & CAB & CB & D \end{bmatrix} \end{aligned} \tag{7}$$

As long as $pm \geq n$, an interaction matrix M exists for an observable system such that $A^p + MO_{\text{bs}_p} = 0$. Existence of interaction matrix M ensures that for $k \geq 0$, Equation (5) can be made state variable independent as:

$$x(k+p) = \left(C_{\text{ont}_p} + MT_{\text{op}_p}\right)u_p(k) - My_p(k) \tag{8}$$

Shifting the time indices by p time steps

$$x(k) = \left(C_{\text{ont}_p} + MT_{\text{op}_p}\right)u_p(k-p) - My_p(k-p) \tag{9}$$

By repeated substitution, for some $q \geq 0$

$$x(k+q) = A^q x(k) + C_{\text{ont}_q} u_q(k) \tag{10}$$

Substituting Equation (9) into Equation (10) yields

$$\begin{aligned} x(k+q) = {} & A^q\left(C_{\text{ont}_p} + MT_{\text{op}_p}\right)u_p(k-p) \\ & - A^q My_p(k-p) + C_{\text{ont}_q} u_q(k) \end{aligned} \tag{11}$$

Multiplying Equation (11) by C gives the output equation as:

$$\begin{aligned} y(k+q) = {} & CA^q\left(C_{\text{ont}_p} + MT_{\text{op}_p}\right)u_p(k-p) \\ & - CA^q My_p(k-p) + \left[CC_{\text{ont}_q}, D\right]u_{q+1}(k) \end{aligned} \tag{12}$$

where $C_{\text{ont}_q} = [A^{q-1}B, \ldots, AB, B]$ and

$$u_p(k-p) = \begin{bmatrix} u(k-p) \\ u(k-p+1) \\ \vdots \\ u(k-1) \end{bmatrix}, \quad y_p(k-p) = \begin{bmatrix} y(k-p) \\ y(k-p+1) \\ \vdots \\ y(k-1) \end{bmatrix},$$

$$u_{q+1}(k) = \begin{bmatrix} u(k) \\ u(k+1) \\ \vdots \\ u(k+q) \end{bmatrix} \tag{13}$$

The output Equation (12) can be written in the standard form as:

$$y(k+q) = \sum_{i=1}^{p} \alpha_i y(k-i) + \sum_{i=1}^{p} \beta_i u(k-i) + \sum_{i=0}^{q} \gamma_i u(k+i) \tag{14}$$

where $[\alpha_p, \ldots, \alpha_2, \alpha_1] = -CA^qM$, $[\beta_p, \ldots, \beta_2, \beta_1] = CA^q(C_{\text{ont}_p} + MT_{\text{op}_p})$ and $[\gamma_0, \gamma_1, \ldots, \gamma_{q-1}] = CC_{\text{ont}_q}, \gamma_q = D$.

Equation (14) is a multistep-ahead predictor where, q step-ahead output is predicted using past p inputs, past p outputs, and future q inputs. Increasing the prediction horizon (q step-ahead output prediction) increases the number of coefficients γ required in Equation (14) to predict the q step-ahead output. Coefficients $\gamma = [CA^{q-1}B, \ldots, CAB, CB, D]$ in Equation (14) are impulse response terms of the system in state space and are known as Markov parameters. During simulations in this article, coefficients α_i, β_i, and γ_i in Equation (14) are obtained directly from a set of input–output data as shown below

$$\left[\rho_1 \vdots \rho_2 \vdots \left[CC_{\text{ont}_q}, D\right]\right] = Y_1 V_1^+ \tag{15}$$

where $\rho_1 = -CA^qM$ and $\rho_2 = CA^q(C_{\text{ont}_p} + MT_{\text{op}_p})$.

V_1^+ denotes the pseudo-inverse of

$$Y_1 = \begin{bmatrix} y_p(p+q) & y_p(p+q+1) & \cdots & y_p(p+q+l) \end{bmatrix} \tag{16}$$

and

$$V_1 = \begin{bmatrix} u_p(0) & u_p(1) & \cdots & u_p(l) \\ y_p(0) & y_p(0) & \cdots & y_p(l) \\ u_{q+1}(p) & u_{q+1}(p+1) & \cdots & u_{q+1}(p+l) \end{bmatrix} \tag{17}$$

The error function for tracking of member stiffness and detection of the extent of structural damage (Level 3 newly developed in this article), are computed, as shown in Figure 1(b). For real time structural damage localization using the ARMarkov observer approach, all damage scenarios need to be considered resulting in a large bank of ARMarkov observers. The focus of this study is to apply ARMarkov observers to determine the extent of damage; it is assumed that structural damage localization (Level 1 and Level 2) is already carried out in real time. Koh et al. (2005b) have proposed one such method where damage in members in a structure is detected and located in real time. The input error functions for real time structural damage localization (Level 1 and Level 2 from Koh et al., 2005b) are computed as shown in Figure 1(a). In this method, an error function corresponding to ith member is of the form:

$$e_i(k) = \sum_{i=0}^{p} \alpha_i y(k-i) + \sum_{i=1}^{p} \beta_i u(k-i) \tag{18}$$

For a system of nth order, each coefficient $\alpha_0, \alpha_1, \ldots, \alpha_p$ is a $1 \times n$ row vector whereas each coefficient $\beta_1, \beta_2, \ldots, \beta_p$ is a scalar. For the ith member, these coefficients are related to those of the original state space model by

$$[\alpha_p, \alpha_{p-1}, \ldots, \alpha_1, \alpha_0] = \left[N_i^T CM_i, N_i^T\right]$$
$$[\beta_p, \beta_{p-1}, \ldots, \beta_2, \beta_1] = \left[N_i^T\left(CC_{\text{ont}_p i} + CM_i T_{\text{op}_p i}\right), N_i^T D_i\right] \tag{19}$$

where N_i is a row vector that is orthogonal to all remaining column vectors D_j, $j \neq i$ such that

$$N_i^T(D_j) = 0, \quad \forall j \neq i \tag{20}$$

First, the location of the damaged structural member is identified using the input error function developed by Koh et al. (2005b) as shown in Figure 1(a). Then, numerous damage scenarios are developed by reducing the stiffness of the damaged member at different levels. Next, input data, denoted as U in Figure 1(b) is used to estimate the response of the structure based on Equation (14) through predetermined ARMarkov observers. Damage scenario 1 denoted as ARMarkov Observer 1 as shown in Figure 1(b), is defined by assuming the extent of damage in certain members of the structure. Corresponding to this ARMarkov Observer 1, coefficients α_i, β_i, and γ_i in Equation (14) are obtained and are used to predict the output of the system. Error, $e1$, is computed by comparing the predicted output and the measured output, denoted as Y in Figure 1(b). Similar errors, $e2, \ldots, en$, are computed as shown in Figure 1(b). When the actual damage scenario is close to the damage scenario represented by ARMarkov Observer 1, error, $e1$, is minimum. As shown in Equation (14), the output prediction equation is a simple linear equation and once the coefficients are obtained, the procedure is computationally efficient. It should be noted that for real time structural damage localization (Level 1 and Level 2) a nonzero error (Equation (18)) corresponding to a member indicates damage in that member. For tracking of member stiffness and determining the extent of structural damage (Level 3), a zero error indicates the

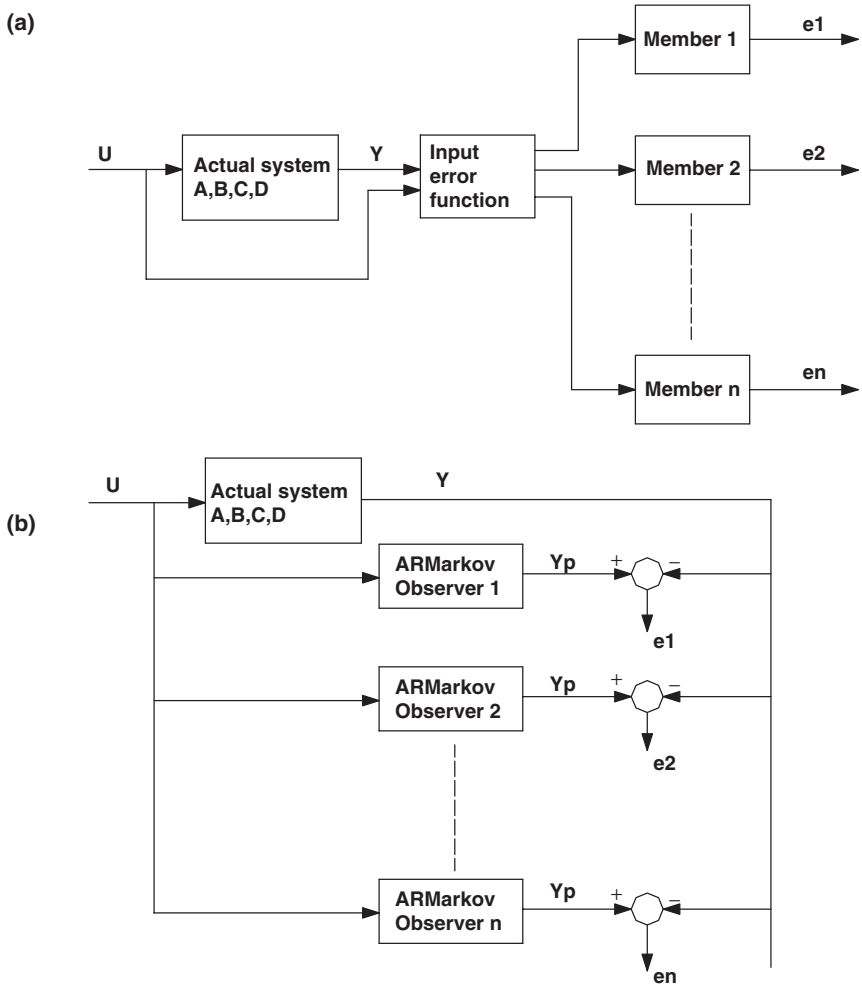

Figure 1. *Block diagram showing error functions for: (a) real time structural damage localization (Level 1 and Level 2) and (b) tracking of member stiffness and determination of the extent of structural damage (Level 3).*

correct observer and the stiffness of the damaged member corresponding to the correct observer is the required true stiffness of the damaged member. Next, the results of the new algorithm are presented for a set of simulations on a three DOF spring–mass–damper system.

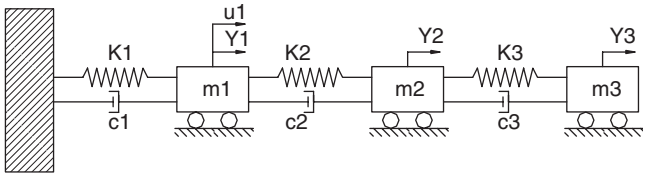

Figure 2. *One-input (u1), three-output (Y1, Y2, Y3) spring–mass–damper system.*

SIMULATION RESULTS AND DISCUSSION

A three DOF spring–mass–damper system is shown in Figure 2. The stiffness of each spring is 100 N/m and mass at each node is 1 kg. Proportional damping is considered, though non-proportional damping can be considered without loss of generality. The system has one input at node 1 ($u1$) and three output sensors (Yi) at nodes 1, 2, and 3 although there is no restriction on the number of inputs. It is assumed that the structural damage detection and localization is already carried out using the input error functions developed by Koh et al. (2005b). Next, the proposed method based on ARMarkov observer is applied to determine the extent of damage. In the following examples once the structure is damaged, it is assumed that the structure regains the healthy state (though not practical) to emphasize the fact that the proposed method can be applied to real time structural health monitoring. The simulation of different stiffness states is performed piecewise linearly. Appropriate properties of the healthy, damaged, and recovered structure are considered in each segment with appropriate initial conditions. In the final example, a more practical case of progressive damage in a critical member of a truss structure and tracking its stiffness change is presented.

Table 1. Damped natural frequencies and damping ratios in each mode.

	System 1		System 2	
	Damped natural frequency (rad/s)	Damping ratio (%)	Damped natural frequency (rad/s)	Damping ratio (%)
Mode 1	4.44	5.62	3.68	56.17
Mode 2	12.47	2.00	12.22	20.05
Mode 3	18.02	1.39	17.85	13.87

Effect of Initial Conditions

To emphasize the significance of initial conditions on structural damage detection, output of damaged structures is considered for two systems, one with small damping ratios (lightly damped) and the other with large damping ratios (highly damped) as listed in Table 1. Damage in the structure is considered by reducing the stiffness of spring 2 ($K2$) by 10%. Damage is introduced in the structure between 2 and 4 s and 6 and 8 s. Thus the structure is healthy between 0 and 2 s, 4 and 6 s, and 8 and 10 s. The output of both systems is predicted using two different approaches (1) six step-ahead prediction using ARMarkov observer and (2) one step-ahead prediction using state space observer, both designed for a healthy structure. The time interval is chosen to demonstrate the advantage of using ARMarkov observers for real time structural damage detection over using a state space observer. The predicted output at node 3 of three DOF system using ARMarkov observer and the state space observer is compared with the measured output, and the error between the predicted output and measured output, is shown in Figure 3. It can be observed from Figure 3(a) that a state space observer continues to show nonzero error function between 4 and 6 s although during this period the structure is healthy. However, ARMarkov observer has a zero error function during this interval and correctly predicts that the structure is healthy. It should be noted that the error function plotted from state space observer steadily decreases, in Figure 3(a), clearly indicating the effect of wrong initial conditions. For a system with high damping ratios, it can be observed from Figure 3(b) that the ARMarkov observer as well as the known state space observer correctly predicts that the structure is healthy during 4–6 s. In this case, due to high damping ratios, effect of initial conditions die out fast; hence, after a few steps, the state space observer predicts the correct zero error function. For ARMarkov observer, the information about exact initial conditions is not very critical because the effect of wrong initial conditions dies out very fast. Thus, for online structural health monitoring of lightly damped flexible structures, the importance of interaction matrix formulation and ARMarkov observers is obvious. Hence, it can be concluded that it is possible to track the stiffness of a member in real time using ARMarkov observers, whereas for state space observers, information about exact initial conditions is important, which is hard to obtain in practice.

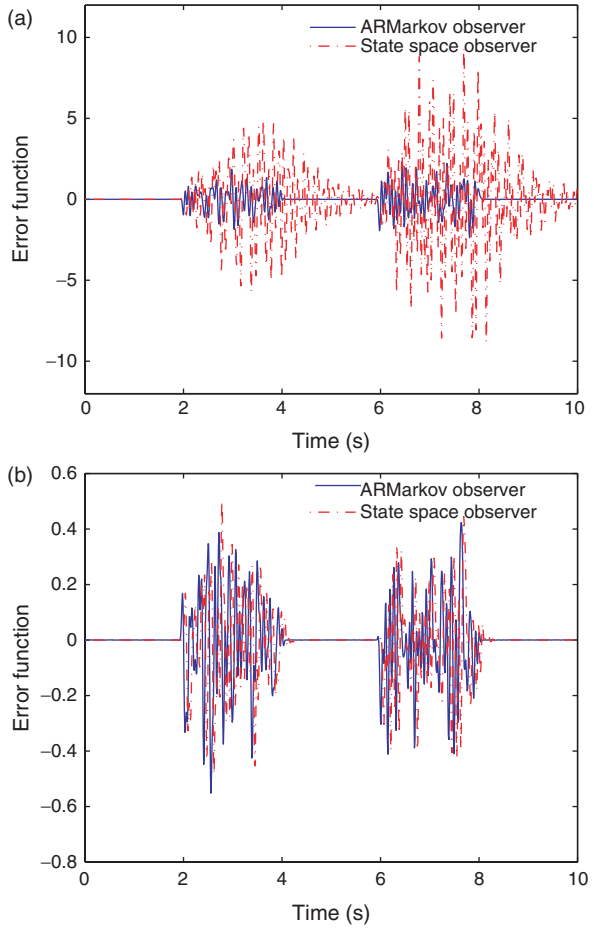

Figure 3. *Effect of initial conditions on ARMarkov observer and state space observer (nonzero error indicates damage): (a) error functions for system 1 (lower damping ratios) and (b) error functions for system 2 (higher damping ratios).*

Extent of Damage

Three DOF spring–mass–damper system is damaged by reducing stiffness of spring 2 ($K2$) from 100 to 75 N/m. A bank of ARMarkov observers is designed for

different values of stiffness for spring 2 ($K2$) and the error between the predicted and measured output at node 3 ($Y3$) is shown in Figure 4. Error functions in Figure 4 correspond to the following ARMarkov observers: (1) Observer 1 designed corresponding to stiffness of springs $K1 = K2 = K3 = 100$ N/m, (2) Observer 2 designed corresponding to stiffness of springs $K1 = K3 = 100$, $K2 = 90$ N/m, (3) Observer 3 designed corresponding to stiffness of springs $K1 = K3 = 100$, $K2 = 80$ N/m, (4) Observer 4 designed corresponding to stiffness of springs $K1 = K3 = 100$, $K2 = 70$ N/m, and (5) Observer 5 designed corresponding to stiffness of springs $K1 = K3 = 100$, $K2 = 60$ N/m. Coefficients α_i, β_i, and γ_i in Equation (14) corresponding to each ARMarkov observer are obtained and are used to predict the output of the system. It should be noted that zero error means that the corresponding observer is the correct observer and provides true stiffness for all members. It is clear from Figure 4 that the error is less for the stiffness range of spring 2 ($K2$) between 70 and 80 N/m. Thus, it can be concluded that the true stiffness of $K2$ must lie in the range 70–80 N/m. To know the exact extent of damage, the error function for spring 2 ($K2$) with stiffness ranging from 70 to 80 N/m is shown in Figure 5.

It can be observed from Figure 5 that the error is less for stiffness range of spring 2 ($K2$) between 74 and 76 N/m; hence, the true stiffness of $K2$ must lie between 74 and 76 N/m. The error function for spring 2 ($K2$) with stiffness between 74 and 76 N/m is plotted in Figure 6. The error function is zero corresponding stiffness of spring 2 ($K2$) equal to 75 N/m and correctly identifies the exact stiffness of spring 2 ($K2$). Note the difference in the magnitude of error function in Figures 4–6.

Covariance of the error functions shown in Figure 4 through to 6 are presented in Figure 7(a)–(c) as a function of the stiffness of spring 2 ($K2$). It can be observed that the error function reaches a minimum corresponding to the damaged stiffness of spring 2 ($K2 = 75$ N/m). Depending upon the accuracy of the extent of damage required, more refined observers can be designed. Thus, from Figure 7(a) it can be concluded that spring 2 has lost about 20–30% of its original stiffness, whereas from Figure 7(c) it is clear that the stiffness of spring 2 is 75% of its original stiffness. Accuracy with which stiffness of the damaged member needs to be determined and noise levels in output measurements decide the number of ARMarkov observers required and hence, the size of the filter bank.

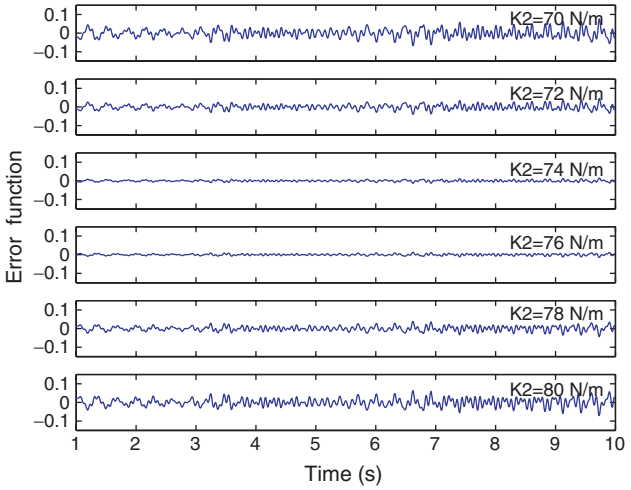

Figure 5. *Error function between predicted and measured output at node 3 (Y3). (Zero error indicates the correct observer and the corresponding stiffness indicates actual stiffness.)*

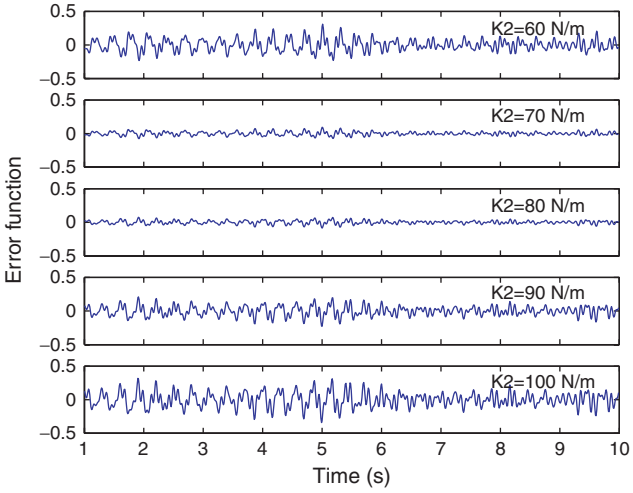

Figure 4. *Error function between predicted and measured output at node 3 (Y3). (Zero error indicates the correct observer and the corresponding stiffness indicates actual stiffness.)*

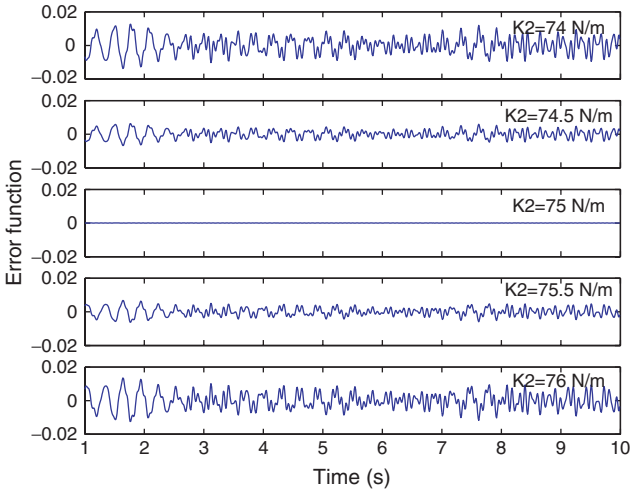

Figure 6. *Error function between predicted and measured output at node 3 (Y3). (Zero error indicates the correct observer and the corresponding stiffness indicates actual stiffness.)*

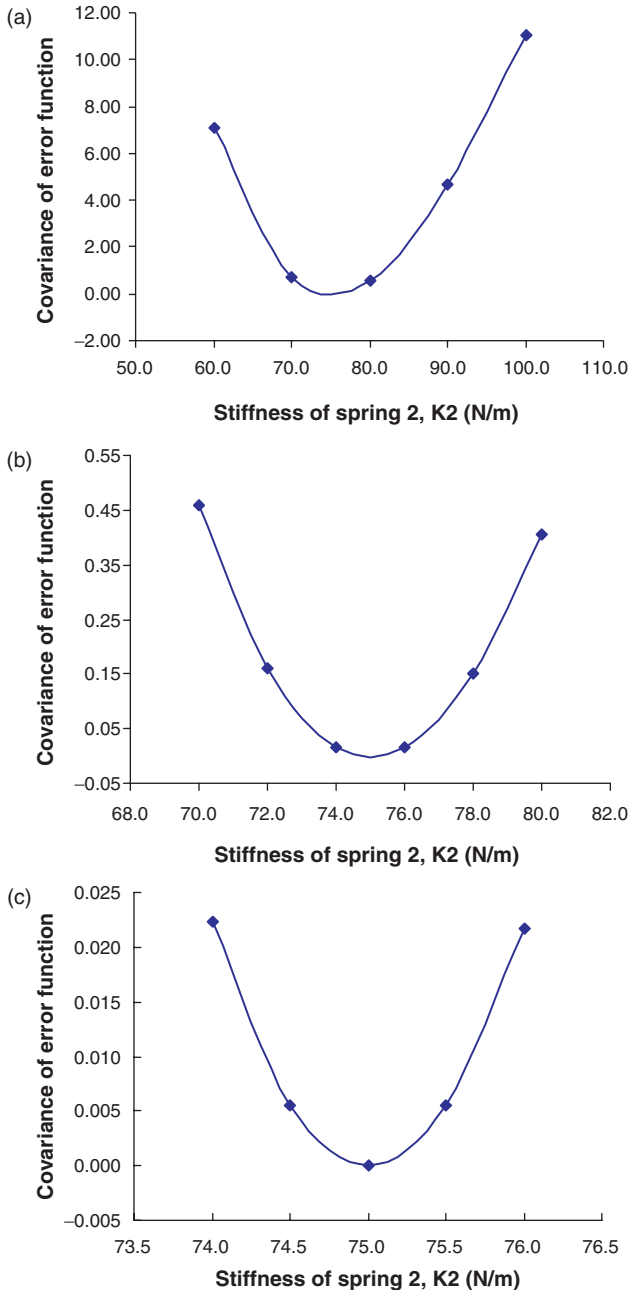

Figure 7. *Covariance of error functions at node 3 (Y3) as a function of stiffness of spring 2 (K2): (a) covariance of error functions in Figure 4; (b) covariance of error functions in Figure 5; and (c) covariance of error functions in Figure 6.*

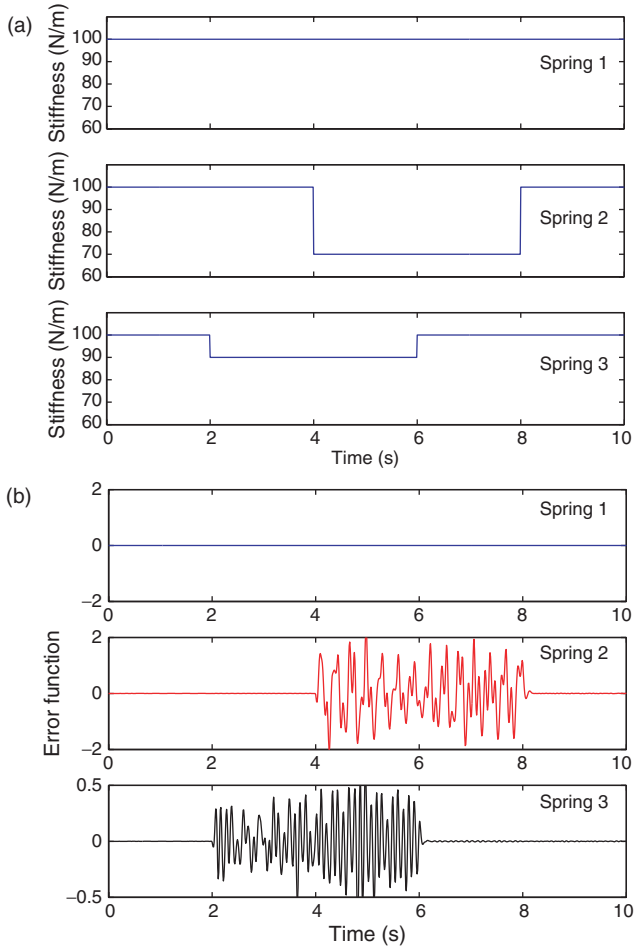

Figure 8. *(a) Stiffness variation in springs and (b) real time localization of damage. (Nonzero error indicates damage.)*

Structural Health Monitoring

In the last section, it was shown that it is possible to capture true stiffness of a damaged member. Now, the proposed method is applied for structural health monitoring study where damage in multiple members is considered. Figure 8(a) shows the stiffness variation for three springs in real time. First, the structure is assumed to be undamaged for 2 s after which stiffness of spring 3 ($K3$) is reduced by 10%. After 4 s, the stiffness of spring 2 ($K2$) is reduced to 70% of the original stiffness. After 6 s, the stiffness of spring 3 ($K3$) is recovered. After 8 s, the stiffness of spring 2 ($K2$) is recovered; and hence the structure has fully recovered its healthy state. Thus, between 4 and 6 s, spring 3 ($K3$) as well as spring 2 ($K2$) are damaged. Figure 8(b) shows the real time damage localization and confirms that between 4 and 6 s both spring 2 ($K2$) and spring 3 ($K3$) are damaged.

Error functions for measurement at node 3 ($Y3$) corresponding to ARMarkov observers designed for different stiffness values of springs are plotted in Figure 9(a)–(o). A zero error function between 2 and 4 s for observer corresponding to $K1 = K2 = 100$ N/m and $K3 = 90$ N/m in Figure 9(i) correctly identifies true stiffness of spring 3 ($K3$). After 4 s, spring 2 is damaged. Since correct stiffness of the spring 3 ($K3$) has already been determined, a bank of ARMarkov observers for different values of stiffness for spring 2 ($K2$) are designed and error functions are plotted in Figure 9(k) through 9(o). A zero error function corresponding to $K2 = 70\%$ during this period as shown in Figure 9(m)

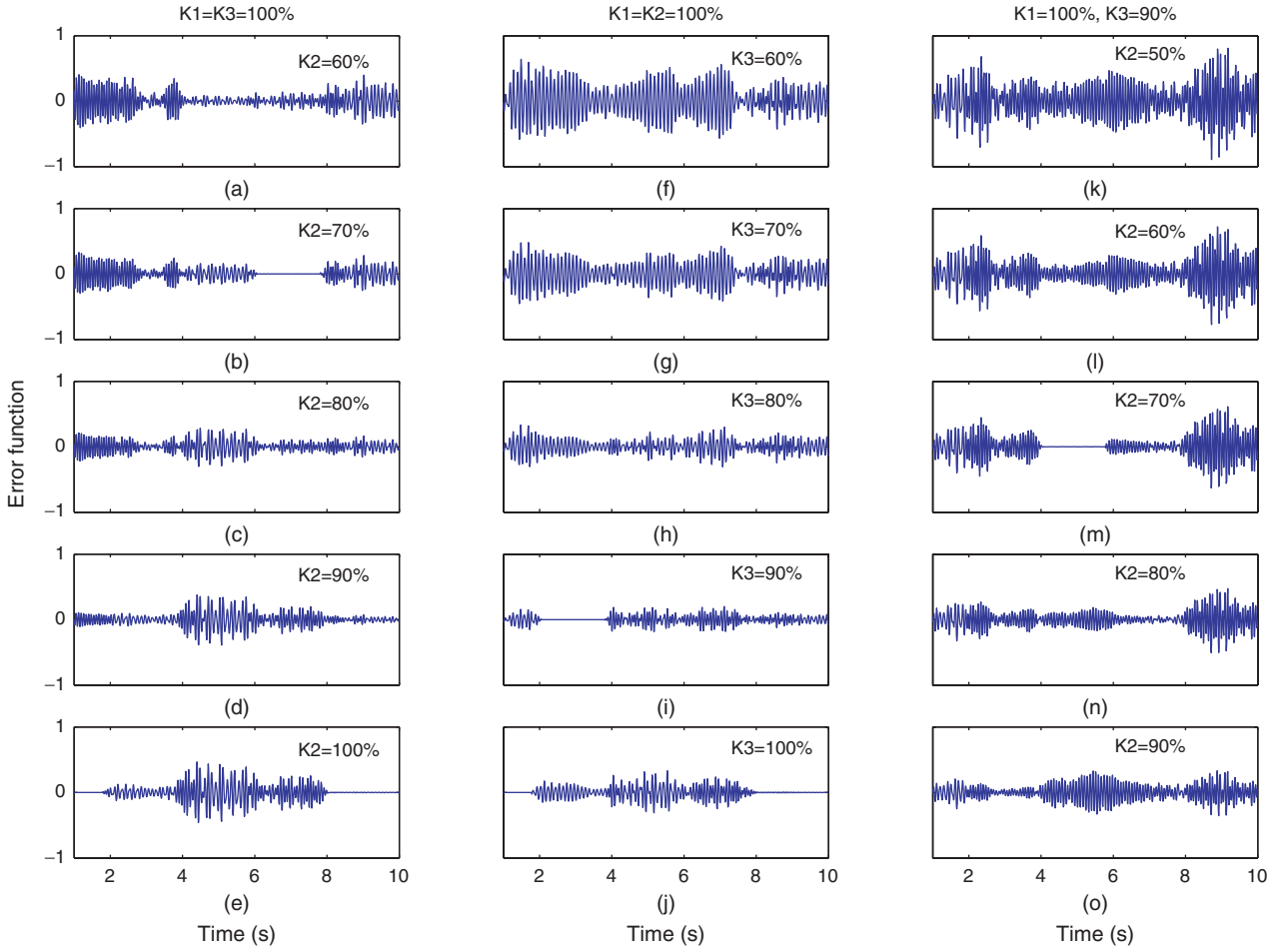

Figure 9. *Error functions for different combinations of ARMarkov observers. (Zero error indicates the correct observer and the corresponding stiffness indicates actual stiffness.)*

correctly indicates that stiffness of spring 2 ($K2$) is 70 N/m. Also, from Figure 9(b), it can be concluded that stiffness of springs between 6 and 8 s are $K1 = 100$ N/m, $K2 = 70$ N/m, and $K3 = 100$ N/m. Thus, it is possible to perform structural health monitoring using the proposed method even in multiple damage scenarios. However, damage occurring in multiple members at different time instants requires a large bank of ARMarkov observers.

Sensitivity of the Structural Damage

Sensitivity to structural damage is an important issue as it is very difficult to identify damage in structures if the change in stiffness for structural members is small. In frequency domain, shift in the natural frequencies is very small, while, in time domain the difference between damaged and healthy structures response is negligible. Ray and Tian (1999) have applied damage sensitive pole placement technique through feedback control gain to enhance the sensitivity of the closed loop natural frequency to structural damage. A large shift in natural frequencies results in large changes in the damaged structure's response and is distinguishable from the healthy structure's response. In this section, a control-based structural damage detection metrics is presented that exploits the closed-loop sensitivity on system parameter perturbations. To illustrate the principle of sensitivity enhancing control (SEC), a single-degree-of-freedom (SDOF) system is presented. The open loop dynamics and undamped natural frequency sensitivity to small change in stiffness and mass of the system are shown as follows:

$$\begin{bmatrix} \dot{x}(t) \\ \ddot{x}(t) \end{bmatrix} = \begin{bmatrix} 0 & 1 \\ -k/m & -b/m \end{bmatrix} \begin{bmatrix} x(t) \\ \dot{x}(t) \end{bmatrix} + \begin{bmatrix} 0 \\ 1/m \end{bmatrix} u(t) \quad (21)$$

$$\frac{\partial \omega_n}{\partial k} = \frac{\omega_n}{2k}, \qquad \frac{\partial \omega_n}{\partial k} = -\frac{\omega_n}{2m} \quad (22)$$

where k, m, b are stiffness, mass, and damping coefficients, respectively, u is an input force. Here, the undamped natural frequency of SDOF system, $\omega_n = \sqrt{k/m}$. It is obvious from Equation (22) that the

sensitivity of undamped natural frequency is a function of system parameter ω_n itself. For example, 1% perturbation in stiffness causes 0.5% change in modal frequency. The goal of SEC is to increase the change of undamped natural frequency to more than 0.5% even with the same 1% change in stiffness. In feedback control of the SDOF system whose state is described by position $x(t)$ and velocity $\dot{x}(t)$, the control input, $u(t) = -[F_1\ F_2][x(t)\ \dot{x}(t)]^T$ can modify the stiffness of the system and in turn change the closed loop undamped natural frequency. In other words, sensitivity enhancement essentially requires a feedback control mechanism that is possible in smart structures. The closed loop system dynamics and undamped natural frequency sensitivity are given by

$$\begin{bmatrix} \dot{x}(t) \\ \ddot{x}(t) \end{bmatrix} = \begin{bmatrix} 0 & 1 \\ -(k+F_1)/m & -(b+F_2)/m \end{bmatrix} \times \begin{bmatrix} x(t) \\ \dot{x}(t) \end{bmatrix} + \begin{bmatrix} 0 \\ 1/m \end{bmatrix} u(t) \tag{23}$$

$$\frac{\partial \omega_{\text{ncl}}}{\partial k} = \frac{\omega_{\text{ncl}}}{2(k+F_1)}, \qquad \frac{\partial \omega_{\text{ncl}}}{\partial k} = -\frac{\omega_{\text{ncl}}}{2m} \tag{24}$$

Thus, the general sensitivity enhancing control concept is to choose control gain that increases the closed loop undamped natural frequency sensitivities to enhance the effect of damage on the dynamic response of a structure. It is apparent from Equation (24) that one should reduce undamped natural frequency of a SDOF system by making F_1 negative to enhance sensitivity to changes in stiffness. Hence, the closed loop sensitivity should be selectively tuned for different types of damage by choosing the appropriate control gain values. The same conclusion can be drawn about the sensitivity of the damped natural frequencies of the system. However, the other gain variable F_2 can be independently used for augmenting the damping of the closed loop system.

Figure 10 shows error functions for an open loop and closed loop (SEC) system at node 1 for a three DOF system shown in Figure 2. Table 2 lists the damped natural frequencies for the open loop and closed loop (SEC) system. In this case, an ARMarkov observer is designed for the healthy state of a structure with SEC and open loop system and the predicted output is compared with the measured output of the corresponding system. Damage in the structure is considered by reducing the stiffness of spring 2 ($K2$) by 10% between 2 and 4 s and 6 and 8 s. Large amplification of an error function can be observed for a system with SEC than for the open loop system. This increased sensitivity to the structural damage helps in identifying the correct ARMarkov observer and the true stiffness of the member. Similar observations can be made from error functions at nodes 2 and 3. In this study, single input

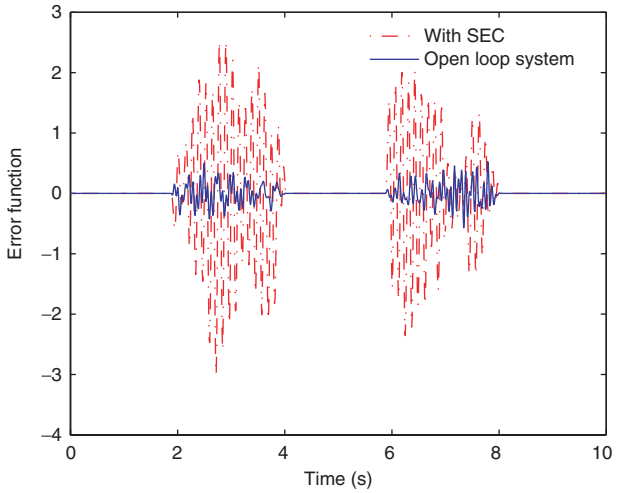

Figure 10. *Error function for closed loop system (with SEC) and open loop system. (Nonzero error indicates damage.)*

Table 2. Damped natural frequencies of open loop and SEC closed loop system.

	Damped natural frequency (rad/s)	
	Open loop	**SEC closed loop**
Mode 1	3.68	1.45
Mode 2	12.22	10.47
Mode 3	17.85	14.02

is used and control gain for pole placement can be uniquely determined for the single input case. However, for the multiple input case, an infinite number of gain sets are possible for a given set of closed loop poles. For multi-input SEC controllers, Koh (2003) has employed eigen structure assignment method (Juang et al., 1989) to enhance the ability to localize damage in smart structures. Thus, it can be concluded that the SEC algorithm can easily be incorporated into the proposed method resulting in increased sensitivity for small structural damages.

Effect of Noise

Noise is an unwanted signal in output measurements but still unavoidable in real structure response. To consider the effect of noise, 5% rms white noise is added to the output of the system. Damage in the structure is considered by reducing the stiffness of spring 2 ($K2$) by 10% between 2 and 4 s and 6 and 8 s. In this case, ARMarkov observer is designed for healthy state of a structure and error functions at node 1 for a three DOF system in Figure 2 are presented in Figure 11. Similar conclusions can be drawn from error functions at nodes 2 and 3. It can be observed from Figure 11 that when the prediction horizon is 10 i.e., predicting 10 steps-ahead

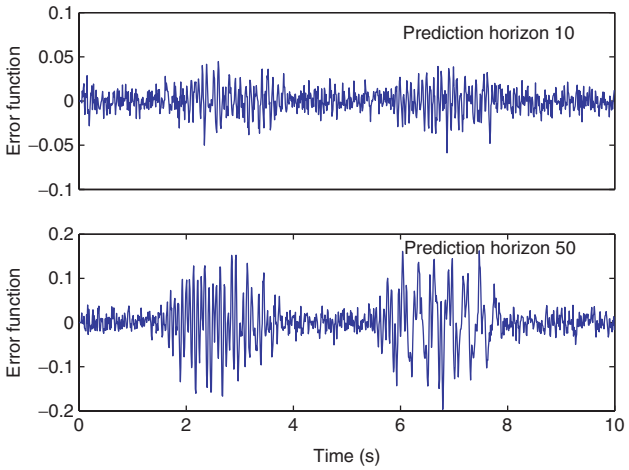

Figure 11. *Error function for open loop system with 5% rms noise in output. (Nonzero error indicates damage.)*

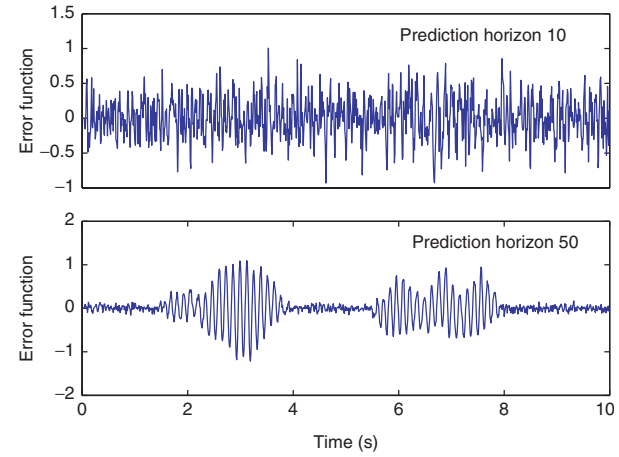

Figure 12. *Error function for closed loop system (with SEC) with 5% rms noise in output. (Nonzero error indicates damage.)*

output, it is difficult to distinguish between error due to structural damage and error due to noise in output measurements. Increasing prediction horizon results in increasing the size of the Hankel matrix to be identified. In the case of noisy output measurements, increasing the size of the Hankel matrix helps in better prediction of the output and reduces the error due to noise in output measurements when compared with error due to structural damage. Using 50 steps-ahead output prediction, it is possible to distinguish between the error due to noise and the error due to structural damage as shown in Figure 11. Thus by adjusting the prediction horizon, better prediction of the output can be achieved with noisy output measurements, which makes it easy to identify the correct observer and in turn the true stiffness of the member. Similar observations can be made for a closed loop system with SEC, as shown in Figure 12.

A Planar Truss Structure

An analytical model of planar aluminum truss structure, shown in Figure 13, is considered to validate the structural health monitoring method proposed in this article. This three-bay planar truss model consists of 12 rod elements connected at eight nodes. A schematic diagram of the structure along with the location and direction of physical input (at node 8 in y-direction) and measured output at nodes 4 and 5 in y-direction is shown in Figure 13. The total length of the truss is 1.5 m with each bay being 0.5 m long, and rod elements having a Young's modulus of $E = 7.58 \times 10^7\,\mathrm{N/m^2}$. All the members are 0.1 in. thick hollow tubes with an outer diameter of 0.5 in. Only a limited number of

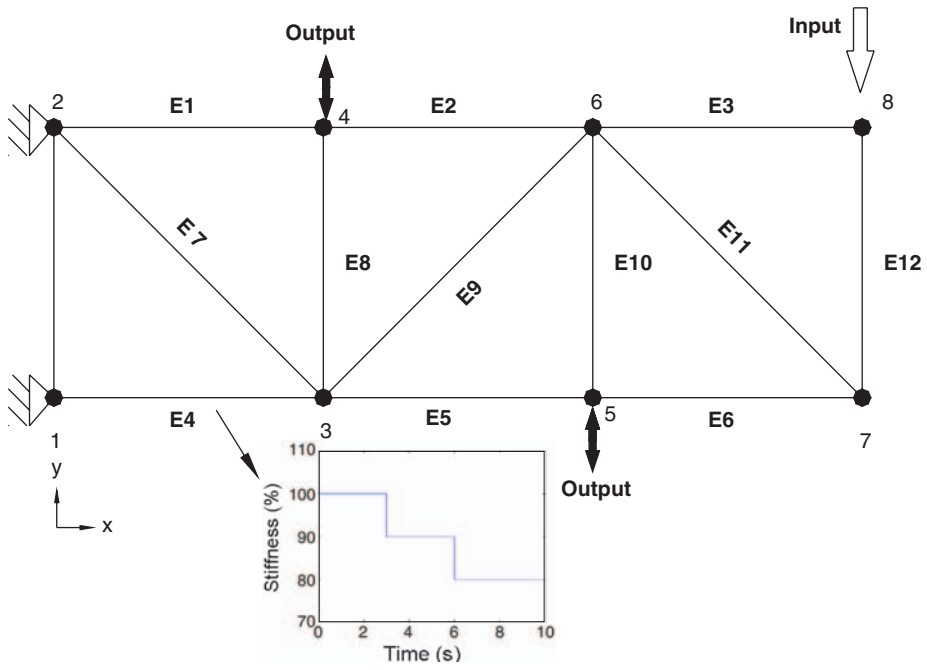

Figure 13. *Aluminum truss structure with one input and two outputs in the y-direction. Also shown is the variation in stiffness of member E4.*

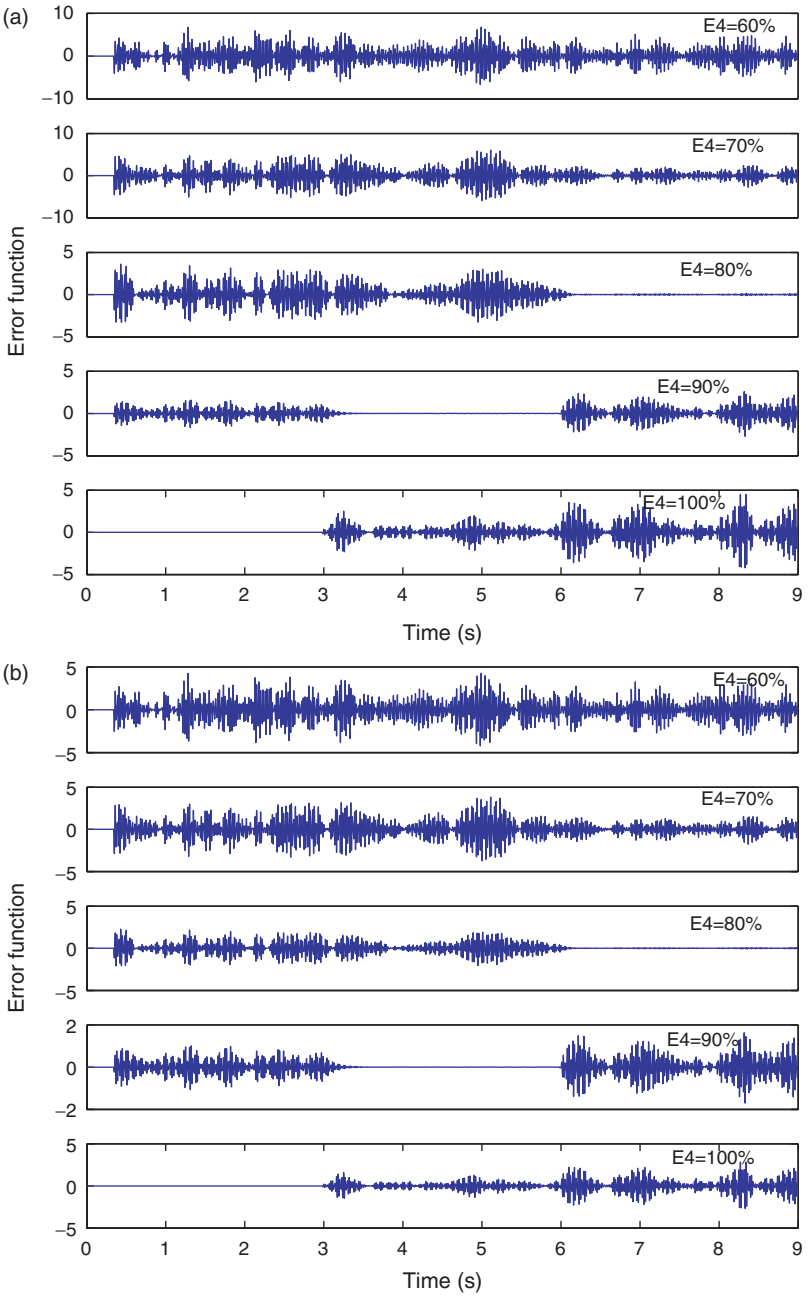

Figure 14. *Error function between predicted and measured output at (a) node 4 and (b) node 5. (Zero error indicates the correct observer and the corresponding stiffness for which observer is designed indicates actual stiffness.) (a) Error functions at node 4 and (b) error functions at node 5.*

displacement sensors are considered to emphasize the fact that the proposed method works even with a limited number of sensors. Stiffness of the member E4 is reduced by 10% after 3 s and is reduced by 20% after 6 s, as shown in Figure 13. This is a more practical case of structural damage where progressive damage in a member is considered. Here, it is assumed that structural damage detection and localization is performed already and damage in member E4 is confirmed. So the task left is to determine the extent of damage (Level 3) and track change in stiffness in member E4. Thus, a number of ARMarkov observers are designed for different stiffness values of member E4 and error functions between the measured outputs, and predicted outputs from ARMarkov observers are plotted as shown in Figure 14. An error function corresponding to E4 = 90% represents an error function plotted from predicted output using an ARMarkov observer designed for stiffness of member E4 equal to 90% of the original stiffness. Zero error function corresponding to E4 = 90% stiffness between 3 and 6 s confirms the correct ARMarkov observer during this period and indicates that member E4 has lost 10% stiffness. Similarly, a zero error function corresponding to E4 = 80% between 6 and 9 s confirms that during this period, the damage in member E4 is 20% stiffness. Thus, it can be concluded that the proposed method can be applied to real structures to track stiffness change

in a member. The method works well even with a limited number of output measurements and will perform well even for highly coupled systems.

CONCLUSIONS

From the results presented in this article, it can be concluded that it is possible to determine the extent of damage (Level 3) in a member and track the stiffness of the damaged member using ARMarkov observers. The number of ARMarkov observers depends upon the accuracy with which the stiffness of the damaged member needs to be determined and noise levels in output measurements. Exact initial conditions are not critical due to interaction matrix formulation used in the ARMarkov observers. Prior knowledge about the process and measurement noise is not required in designing ARMarkov observers. The proposed method works well even with noisy measurements and by adjusting the prediction horizon parameter, it is possible to differentiate between the error due to noise in output measurements and error due to structural damage. Closed-loop feedback control (SEC) algorithm can be easily incorporated into the proposed method enhancing sensitivity to structural damage. The proposed method works well even when a limited number of output measurements are available. Although the proposed method has the aforementioned advantages over existing observer based methods, it suffers from the limitation of observer based methods that it needs a large bank of ARMarkov observers for multiple damage cases.

ACKNOWLEDGMENTS

The authors wish to acknowledge the support of the Texas Institute for the Intelligent Bio-Nano Materials and Structure for Aerospace Vehicles, funded by NASA Cooperative Agreement No. NCC-1-02038.

REFERENCES

Adams, R.D., Cawley, P., Pye, C.J. and Stone, B.J. 1978. "A Vibrational Technique for Non-destructively Assessing the Integrity of Structures," *Journal of Mechanical Engineering Science*, 20:93–100.

Armon, D., Ben-Haim, Y. and Braun, S. 1994. "Crack Detection in Beams by Rank-ordering of Eigenfrequency Shifts," *Mechanical Systems and Signal Processing*, 8:81–91.

Beard, R.V. 1971. Failure Accommodation in Linear Systems through Self Reorganization, PhD Dissertation, Department of Aeronautics and Astronomics, Massachusetts Institute of Technology, MA, USA.

Cornwell, P., Kam, M., Carlson, B., Hoerst, B., Doebling, S. and Farrar, C.R. 1998. "Comparative Study of Vibration-based Damage ID Algorithms," In: *International Modal Analysis Conference*, pp. 1710–1716.

Darling, S. and Phan, M.Q. 2004a. "Dynamic Output Feedback Predictive Controllers for Vibration Suppression and Periodic Disturbance Rejection," In: *Proceedings of the 14th AAS/AIAA Space Flight Mechanics Conference*, Maui, HI.

Darling, S. and Phan, M.Q. 2004b. "Predictive Controllers for Simultaneous Tracking and Disturbance Rejection," In: *Proceedings of the AIAA Conference on Guidance, Navigation, and Control*, AIAA-2004-5109, Providence, RI, August 2004.

Doebling, S.W., Farrar, C.R., Prime, M.B. and Shevitz, D.W. 1996. Damage Identification and Health Monitoring of Structural and Mechanical Systems from Changes in Their Vibration Characteristics: A Literature Review, Los Alamos National Laboratory Report.

Goodzeit, E. and Phan, M.Q. 2000. "System Identification in the Presence of Completely Unknown Periodic Disturbances," *Journal of Guidance, Control, and Dynamics*, 23(2):251–259.

Hjelmstad, K.D. and Shin, S. 1995. "Crack Identification from Modal Response," *Journal of Sound and Vibration*, 198:527–545.

Jones, H.L. 1973. Failure Detection in Linear Systems, PhD Dissertation, Massachusetts Institute of Technology, MA, USA.

Juang, J.-N., Lim, K.B. and Junkins, J.L. 1989. "Robust Eigensystem Assignment for Flexible Structures," *Journal of Guidance, Control and Dynamics*, 12(3):381–387.

Kam, T.Y. and Lee, T.Y. 1992. "Detection of Cracks in Structures using Modal Test Data," *Engineering Fracture Mechanics*, 42(2):381–387.

Koh, B.-H. 2003. Damage Detection of Smart Structures through Sensitivity Enhancing Control, PhD Dissertation, Thayer School of Engineering, Dartmouth College, NH, USA.

Koh, B.-H., Li, Z., Dharap, P., Nagarajaiah, S. and Phan, M.Q. 2005a. "Actuator Failure Detection using Interaction Matrix Formulation," *Journal of Guidance, Control, and Dynamics*, 28(5):895–901.

Koh, B.-H., Dharap, P., Nagarajaiah, S. and Phan, M.Q. 2005b. "Real-Time Structural Damage Monitoring by Input Error Function," *AIAA Journal*, 43(8):1808–1814.

Kranock, S.J. 2000. *Real-time Structural Damage Detection Using Model-Based Observers*, PhD Dissertation, Department of Aerospace Engineering Science, University of Colorado, Boulder, Co, USA.

Liberatore, S., Speyer, J.L. and Hsu, A.C. 2003. "Fault Detection Filter Applied to Structural Health Monitoring," In: *Proceedings of the 42nd IEEE Conference on Decision and Control*, Hawai, USA.

Lim, R.K. and Phan, M.Q. 1997. "Identification of a Multistep-Ahead Observer and Its Application to Predictive Control," *Journal of Guidance, Control and Dynamics*, 20(6):1200–1206.

Lim, R.K., Phan, M.Q. and Longman, R.W. 1998. State Estimation with ARMarkov Models, Department of Mechanical and Aerospace Engineering Technical Report No. 3046, Princeton University.

Phan, M.Q., Lim, R.K. and Longman, R.W. 1998. Unifying Input-output and State-space Perspectives of Predictive Control, Department of Mechanical and Aerospace Engineering Technical Report No. 3044, Princeton University.

Ray, L.R. and Tian, L. 1999. "Damage Detection in Smart Structures through Sensitivity Enhancing Feedback Control," *Journal of Sound and Vibration*, 227(5):987–1002.

Rytter, A. 1993. Vibration Based Inspection of Civil Engineering Structures, Department of Building Technology and Structural Engineering, PhD Thesis, Aalborg University, Denmark.

Seibold, S. and Weinert, K. 1996. "A Time Domain Method for the Localization of Cracks in Rotors," *Journal of Sound and Vibration*, 195(1):57–73.

Stubbs, N., Kim, J.T. and Farrar, C.R. 1995. "Field Verification of a Nondestructive Damage Localization and Severity Estimation Algorithm," In: *Proceedings of the 13th International Modal Analysis Conference*, pp. 210–218.

Tasker, F., Dunn, B. and Fisher, S. 1999. "Online Structural Damage Detection using Subspace Estimation," In: *Proceedings of the 1999 IEEE Aerospace Conference*, Snowmass, Colorado, CD-ROM Edition, Track 3, Paper 3.402.